Temperature dependence of photoluminescence property in BaIn$_2$O$_4$

Huiyong Deng (邓惠勇)[1*], Qiwei Wang (王奇伟)[1], Ping Ren (任　平)[2], Jie Wu (吴　杰)[1],
Junchao Tao (陶俊超)[1], Xin Chen (陈　鑫)[1], and Ning Dai (戴　宁)[1]**

[1]*National Laboratory for Infrared Physics, Shanghai Institute of Technical Physics,*
Chinese Academy of Sciences, Shanghai 200083, China

[2]*Department of Energy Sources and Environment Engineering, Shanghai University of Electric Power, Shanghai 200090, China*

[*]Corresponding author: hydeng@mail.sitp.ac.cn; [**]corresponding author: ndai@mail.sitp.ac.cn

The temperature-dependent photoluminescence (PL) spectra of BaIn$_2$O$_4$, prepared by coprecipitation, are measured and discussed. Aside from the reported 3.02-eV violet emission, the 1.81-eV yellow emission involved with oxygen vacancy is also observed at room temperature wherein the deep donor level is at 1.2 eV. With the temperature increasing, the peak energies for both emissions show a red shift. Moreover, the yellow emission intensity decreases while the violet emission intensity increases. The temperature dependence of the yellow emission intensity fits very well into the one-step quenching process equation, indicating a fitted activation energy at 19.2 meV.

OCIS codes: 000.2190, 160.4760, 160.6000.
doi: 10.3788/COL201109.011602.

High-efficiency visible-light photocatalysts have drawn increasing attentions due to their potential applications in splitting water to produce hydrogen and degenerating organic pollutants, which will alleviate the energy crisis and impending environmental pollution[1,2]. Since Zou *et al.* found that In$_{1-x}$Ni$_x$TaO$_4$ ($x = 0-0.2$) could directly split water under visible light[3], various oxide semiconductors have been developed[4,5], among which barium indium oxide compounds, particularly BaIn$_2$O$_4$ and Ba$_2$In$_2$O$_5$, have been considered important[6−8]. High-efficiency photocatalysts are usually selected if the lower limit of their conduction band is higher than the redox potential of H$^+$/H$_2$, and the upper limit of their valence conduction is lower than the redox potential of O$_2$/H$_2$O. Hence, an understanding of the band structures of these semiconductors is necessary for assigning their applications effectively. BaIn$_2$O$_4$ has an indirect band gap of 2.73 eV at room temperature, which has been measured by Yin *et al.*[9]. However, further research has been unavailable. In this letter, the BaIn$_2$O$_4$ tablet is prepared using coprecipitation and the temperature-dependence of its photoluminescence (PL) spectra is investigated. Aside from the reported violet emission, the yellow emission involved in oxygen vacancy is also observed and analyzed.

Ba(NO$_3$)$_2$ (reagent grade) and In(NO$_3$)$_3$·5H$_2$O (reagent grade) were used as the barium and indium sources. Na$_2$CO$_3$ (reagent grade) and NaOH (reagent grade) were used as the precipitators to respectively react with Ba(NO$_3$)$_2$ and In(NO$_3$)$_3$ to form the BaCO$_3$ and In(OH)$_3$ precipitates, respectively. First, 250 mL of a mixed aqueous solution of 0.088-mol/L Ba(NO$_3$)$_2$ and 0.16-mol/L In(NO$_3$)$_3$ was slowly added to a 600-mL mixed solution of 0.08-mol/L Na$_2$CO$_3$ and 0.33-mol/L NaOH under mechanical agitation for 1 h. After the precipitates formed, the precursor powders were obtained through pumping filtration and washing until the pH of the washing solution was 7. Next, the precursors were

dried at 100 °C for about 2 h and then presintered in a corundum crucible at 900 °C for 1.5 h. After cooling to room temperature, the mixtures were pressed into a circular tablet with a 10-mm diameter and 2-mm thickness. Finally, the tablet was again placed in the corundum crucible and sintered at 1100 °C for 3 h.

X-ray diffractometry (XRD) was performed using a X-ray diffractometer (D/max 2550, Rigaku, Japan) with Cu Kα radiation at a scan rate of 5°/min. The surface morphology of the tablet sample was observed using a scanning electron microscope (SEM) (Sirion200D1615, FEI, USA). The accelerating voltage was 20 kV, the spot size was 3 nm, and the working distance was 5 μm. The PL spectra were recorded by spectrometer (SP2500i, PI/Acton, USA) using a 266-nm laser set to 10 mW.

Figure 1 shows the measured XRD pattern of the sample, which exhibits fine structures near $2\theta = 31°$ (inset). The lattice plane corresponding to each diffraction peak is denoted by the Miller index according to the standard PDF card (number 84-1961) of BaIn$_2$O$_4$, as shown in Fig. 1. The measured diffraction
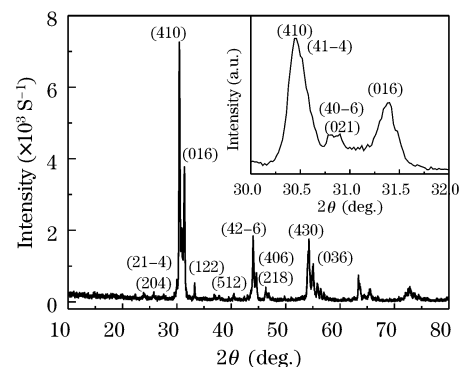

Fig. 1. Measured XRD pattern of BaIn$_2$O$_4$. The diffraction peaks are denoted by Miller indices according to the standard PDF card (number 84-1961). The magnified fine structures near $2\theta = 31°$ are shown in the inset.

peaks agree very well with the standard XRD pattern and no diffraction peaks from other phases are observed, indicating that the obtained sample is pure and has a monoclinic structure. The strong diffraction peaks indicate that the sample is highly crystalline. Figure 2 shows the SEM image of the apparently irregular surface of the sample tablet, mainly composed of block (about 750 nm) and rod-like (about 2 μm) particles. These particles are tightly bound together, such that the interface between the adjacent particles cannot be clearly distinguished. The rough surface morphology weakens the PL intensity to some extent due to the scattering effect.

Figure 3 shows the PL spectra measured at temperatures ranging from 13 to 300 K, from which the spectra are divided into two sections according to emission intensity, as shown in Figs. 3(a) and (b), respectively. The curves in Fig. 3(b) are shifted vertically for clarity. At $T > 100$ K, two well-defined emission peaks are observed. The violet emission peak corresponds to indirect radiation recombination, as reported by Yin *et al.* using the diffuse reflectance spectrum[9]. The observed weak shoulder at the high-energy side indicates thermal population of excited states[10]. From the peak position, the room temperature band gap E_g is 3.02 eV, close to fitting the result by Yin *et al.* (2.73 eV)[9]. However, in Fig. 2 of Ref. [9], the reported E_g at 454 nm was 2.73 eV, which corresponds to the onset of the absorption edge, indicating
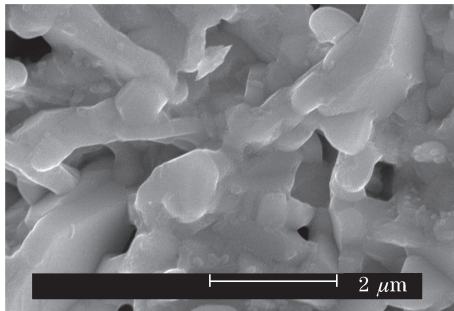

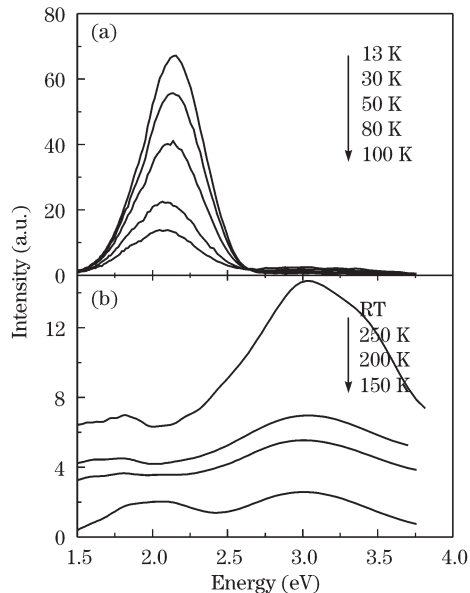Fig. 2. Surface image of the tablet sample under SEM.

Fig. 3. PL spectra of BaIn$_2$O$_4$ recorded at different temperatures. The curves in Fig. 3(b) are shifted vertically for clarity.

that E_g is underestimated. Meanwhile, the measured E_g at 410 nm, 3.02 eV, nearly approaches the wavelength at half-maximum of the absorption edge, about 400 nm. Thus, the E_g measured through PL is more accurate than the reported value through diffuse reflection. Given that the indirect radiation recombination process is accompanied by emission and/or absorption of phonons to satisfy momentum conservation, the involved emission intensity is much weaker than the direct one. This is shown in Fig. 3, in which the intensities in Fig. 3(a) are approximately 10 times stronger than those in Fig. 3(b). With the temperature decreasing, the peak energy of the violet emission shifts indistinguishably towards the higher energy side, however, the emission intensity quickly decreases and is almost quenched at $T < 100$ K due to the reduced phonons. In this experiment, the weak violet emission is not only attributed to the indirect recombination but is also affected by the coarse surface, as shown in Fig. 2.

The weak yellow emission at 1.82 eV observed at room temperature (see Fig. 3(b)) was not observed by Yin *et al.* using diffuse reflectance spectrum[9]. Given that the monoclinic BaIn$_2$O$_4$ has an isotopic structure with other monoclinic AB$_2$O$_4$ compounds such as SrAl$_2$O$_4$[11,12], this emission is analogously assigned to the recombination involved with the oxygen vacancy donor level derived from the empty sp^3-orbitals of B^{3+} ions surrounding the oxygen vacancy. The determined oxygen vacancy level is 1.2 eV lower than the lower limit of the conduction band, indicating that the oxygen vacancy forms the deep donor center and is approximately located in the middle of the band gap. This is similar to the behavior of oxygen vacancy in ZnO[13−16]. With the temperature increasing, the peak energy of the yellow emission evidently shifts towards the lower energy side, but the emission intensity is gradually reduced. The detailed temperature dependence of the peak energy and emission intensity is shown in Fig. 4, in which the solid and empty circles represent the peak energy and the emission intensity, respectively. With the temperature increasing, the peak energy evidently decreases at lower temperatures but slightly changes at $T > 100$ K. This characteristic differs from the temperature-dependence of the electronic interband recombination described by Varshni's empirical equation. The emission intensity has almost the same varying trend as the peak energy, but it has a steeper slope at lower temperatures. To clarify the thermal quenching mechanism involved with the non-radiative recombination, the quenching activation energy E_{act} is derived by the following one-step quenching process equation[17]

$$I_{PL} = \frac{I_0}{1 + C \exp(-E_{act}/k_B T)}, \qquad (1)$$

where I_0 is the emission intensity at 0 K, C is the proportionality constant, k_B is the Boltzmann's constant, and T is the thermodynamic temperature. The solid line in Fig. 4 represents the fitted result, in which the experimental data agrees well with the fitted result. The activation energy E_{act} is 19.2 meV, about one order of magnitude smaller than the thermal depth of donors[18]. Thus, the decreasing intensity of yellow emission is attributed to
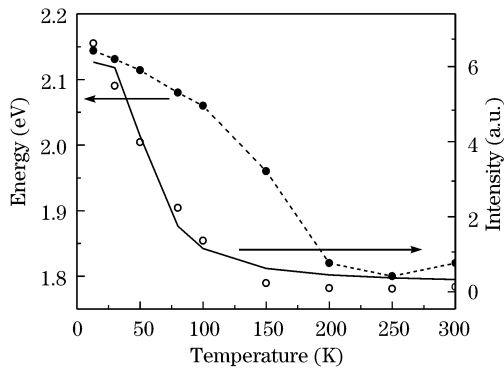
Fig. 4. Temperature dependence of the peak energy and yellow emission intensity for $BaIn_2O_4$.

the thermal detrapping of donor-bound exciton. From Fig. 3, the variation of the full-width at half-maximum (FWHM) of the yellow emission intensity as a function of temperature is also noted. The FWHM increases from 0.478 to 0.585 eV when the temperature changes from 13 to 100 K although no evident change in FWHM is observed at $T > 100$ K due to the weak emission intensity. The corresponding FWHM increases with temperature raising is one of the characteristics of oxygen vacancy in ZnO[14], which also confirms the assignment of the yellow emission.

In conclusion, pure $BaIn_2O_4$ is prepared using coprecipitation. The obtained $BaIn_2O_4$ tablet has a monoclinic structure and is composed of tightly bound block and rod-like particles. Aside from the reported 3.02-eV violet emission corresponding to the indirect recombination, the temperature dependence of the 1.81-eV yellow emission involved with oxygen vacancy level is investigated. Oxygen vacancy forms in the deep donor center and, at room temperature, the donor level is at 1.2 eV. With the temperature increasing, the peak energies for both emissions show a red shift. Moreover, the yellow emission intensity decreases but the violet emission intensity increases. The temperature dependence of the yellow emission intensity fits into the one-step quenching process equation and the fitted activation energy E_{act} is measured to be 19.2 meV.

References

1. M. Ni, M. K. H. Leung, D. Y. C. Leung, and K. Sumathy, Renew. Sust. Energ. Rev. **11,** 401 (2007).
2. Y. Wu, X. Wang, and C. Ma, Acta Opt. Sin. (in Chinese) **28,** 2408 (2008).
3. Z. Zou, J. Ye, K. Sayama, and H. Arakawa, Nature **414,** 625 (2001).
4. Z. Zou, J. Ye, K. Sayama, and H. Arakawa, J. Photochemistry and Photobiology A **148,** 65 (2002).
5. X. Zhang, Z. Ai, F. Jia, L. Zhang, X. Fan, and Z. Zou, Mater. Chem. Phys. **103,** 162 (2007).
6. F. E. Osterloh, Chem. Mater. **20,** 35 (2007).
7. D. Wang, Z. Zou, and J. Ye, Chem. Mater. **17,** 3255 (2005).
8. W. K. Chang, Y. S. Wu, C. Y. Tzeng, and A. Y. Lin, J. Alloys Compounds **478,** 341 (2009).
9. J. Yin, Z. Zou, and J. Ye, J. Mater. Res. **17,** 2201 (2002).
10. S. Sanguinetti, T. Mano, M. Oshima, T. Tateno, M. Wakaki, and N. Koguchi, Appl. Phys. Lett. **81,** 3067 (2002).
11. P. Escribano, M. Marchal, M. Luisa Sanjuán, P. Alonso-Gutiérrez, B. Julián, and E. Cordoncillo, J. Solid State Chem. **178,** 1978 (2005).
12. F. Clabau, X. Rocquefelte, S. Jobic, P. Deniard, M. H. Whangbo, A. Garcia, and T. Le Mercier, Solid State Sci. **9,** 608 (2007).
13. F. Leiter, H. Alves, D. Pfisterer, N. G. Romanov, D. M. Hofmann, and B. K. Meyer, Physica B **340-342,** 201 (2003).
14. P. Klason, T. Moe Børseth, Q. X. Zhao, B. G. Svensson, A. Y. Kuznetsov, P. J. Bergman, and M. Willander, Solid State Commun. **145,** 321 (2008).
15. S. Shi and T. Huang, Chin. Opt. Lett. **8,** 221 (2010).
16. T. Huang, S. Zhou, H. Teng, and H. Lin, Acta Opt. Sin. (in Chinese) **28,** 1420 (2008).
17. A. Zubiaga, J. A. Garcia, F. Plazaola, F. Tuomisto, K. Saarinen, J. Z. Perez, and V. M. Sanjose, J. Appl. Phys. **99,** 053516 (2006).
18. M. Leroux, N. Grandjean, B. Beaumont, G. Nataf, F. Semond, J. Massies, and P. Gibart, J. Appl. Phys. **86,** 3721 (1999).